

1 **Estimating habitat-specific abundance and behavior of several groundfishes using**
2 **stationary stereo still cameras in the southern California Bight**

3

4 Christopher N. Rooper^{1*}, Kresimir Williams¹, Richard H. Towler¹, Rachel Wilborn^{1,2}, Pam
5 Goddard^{1,2}

6

7 ¹Alaska Fisheries Science Center, National Marine Fisheries Service, 7600 Sand Point Way NE,
8 Seattle, WA, 98115, USA

9

10 ²Lynker Technologies, LLC under contract to: Alaska Fisheries Science Center, National Marine
11 Fisheries Service, 7600 Sand Point Way NE, Seattle, WA, 98115, USA

12

13

14 *Current address: Pacific Biological Station, Fisheries and Oceans Canada, 3190 Hammond Bay
15 Road, Nanaimo BC V9T6N7, Canada

16

17 Chris.Rooper@dfo-mpo.gc.ca

18

19

20

21 **Abstract:** The increasing use of underwater cameras to estimate fish abundance often does not
22 account for the behavior of target species. These behaviors can affect detectability of fish and
23 bias density estimates. This study estimated abundance and behavior of several rockfishes
24 (*Sebastes* spp) and lingcod (*Ophiodon elongatus*) at Footprint Bank, a small offshore bank using
25 images from randomly deployed stationary cameras. Deployments collected images at 30-second
26 intervals over ~24 hour periods to examine the behaviors of rockfish that might impact
27 abundance estimates. The results showed that time of day and tidal change had a significant
28 effect on the probability of presence, estimated abundance and species composition of fish, with
29 densities highest for most species during daylight hours. The time elapsed since camera
30 deployment did not have a significant effect on fish density. Fish density was significantly
31 affected by habitat composition, an effect primarily driven by speckled rockfish (*Sebastes ovalis*)
32 which exhibited a 5-fold increase in abundance in bedrock habitats. Speckled rockfish were the
33 most abundant rockfish at depths less than 150 m, with an estimated abundance of 12,994 fish
34 (SE = 6,722) on Footprint Bank. The abundance estimates and coefficients of variation were
35 comparable to surveys conducted in 2011 and 2012 using remotely operated vehicles (ROVs)
36 and manned submersibles. The implications of this study are that habitat and behavior as well as
37 timing of the survey (day/night) are important considerations determining the perceived density
38 of fishes from underwater image surveys.

39

40 **Keywords:** Sebastes; stereo camera; survey design; population estimate; untrawlable habitat;

41 California

42

43

44 **Introduction**

45 Underwater cameras have become an increasingly popular approach to estimate fish
46 abundance for fisheries management as an alternative to extractive techniques (Mallet and
47 Pelletier 2014). Underwater camera surveys have advantages over traditional survey methods
48 such as bottom trawls for documenting rare or endangered species with conservation concerns
49 (e.g. Yoklavich et al. 2007) and for high-relief areas that are not easily sampled using trawls or
50 nets (e.g. Cordue 2007, Rooper et al. 2010).

51 An advantage of traditional survey methods such as bottom trawls is the large volume of
52 research on fish behavior and gear catchability that has previously been conducted and has
53 resulted in better understanding of observed trends. These can include information on gear
54 selectivity of different fish sizes (Huse et al. 2000, Williams et al. 2011, DeRobertis et al. 2017),
55 gear efficiency under varying environmental and fishing conditions (Somerton and Munro 2001,
56 Munro and Somerton 2002, Weinberg 2003, Weinberg and Kotwicky 2008, Kotwicky et al.
57 2009), and behavioral responses to fishing gear (Bublitz 1996, Bryan et al. 2014). This body of
58 literature is useful to interpret and assess catch rates and the resulting indices of abundance for
59 traditional abundance survey methods, such as trawls, longlines, set nets and traps. Because
60 optical-based surveys will have their own sampling properties and biases a similar line of
61 investigation is needed for those gears (Campbell et al. 2015)

62 Comparisons of underwater video surveys to other types of gear, such as baited traps
63 have indicated differences in catchability among gear types (Bacheler et al. 2013, Geraldi et al.
64 2019). These can highlight differences related to behavior, such as size selectivity of some gears
65 (Rooper et al. 2012), differences in spatial patterns of frequency of occurrence (Bacheler et al.
66 2013), and even differences in detectability among different gears or underwater camera systems

67 (Bacheler et al. 2014, Kilfoil et al. 2017). Questions about the influence of environmental factors
68 in availability and detectability in camera surveys have not often been addressed and in addition
69 these effects are often strongly influenced by the behavior of targeted fishes. For instance it has
70 been demonstrated that fish behavior influences fish detectability for underwater camera surveys
71 both in response to transiting underwater vehicles (e.g. Laidig et al. 2013, Somerton et al. 2017),
72 response to stimuli from the vehicle, such as lights or sounds (Lorance and Trenkel 2006, Stoner
73 et al. 2008, Rooper et al. 2015) or due to behaviors such as diurnal migrations (Stanley et al.
74 1999, Rooper et al. 2010) or swimming and schooling behaviors (Bacheler and Shertzer 2015).
75 Fish behaviors can be habitat-specific, such as cryptic or flight response behaviors of some fish
76 in high-relief habitats that influence the ability of detection by cameras (Trenkel et al. 2004,
77 Stone et al. 2015). Therefore, accounting for habitat types in both the abundance estimates and
78 behavior observations is crucial for getting an accurate measure of fish abundance.

79 The primary objective of this study was to estimate the abundance and variance of seven
80 species of common rockfish (*Sebastes* spp.) and lingcod (*Ophiodon elongatus*) in untrawlable
81 habitat using stationary cameras. We also examined factors that influence the perceived density
82 from an underwater camera survey using long-term (24 hour) deployments of stationary cameras.
83 Since the cameras were designed to have minimal impact on the behavior of fishes, we examined
84 environmental influences on patterns of density over 24 hour periods. Specifically we looked at
85 tidal and diel cycles, patterns in the initial arrival time of fishes to the camera, variability in
86 density over long-term deployments and the effects of habitat and depth on density estimates.
87 Ultimately, the goal of this study was to make recommendations for future surveys of rockfishes
88 in untrawlable habitats.

89

90 **Materials and Methods**

91 *Study area*

92 All surveys were conducted on Footprint Bank, a rocky seamount in southern California
93 located at the southern end of the Anacapa Passage (between Santa Cruz and Anacapa Islands) in
94 the Channel Islands National Marine Sanctuary at approximately 33° 54.84' N and 119°28.35'
95 W (Figure 1). Footprint Bank is about 10 km² in area ranging in depth from 80 to 500 m, and
96 generally trends northwest-southeast. The study site is located inside the State and Federal
97 Footprint Marine Reserves. Footprint Bank consists of high-relief outcrops, sand flats, and
98 cobble fields and hosts a diverse assemblage of groundfishes (Schroeder and Love, 2002;
99 Yoklavich et al., 2013). The area surveyed for this project consisted largely of rocky habitat from
100 90-150 m depth which reduced the surveyed area to 4.8 km² (Figure 1). In total, 50 stations were
101 chosen randomly within this depth range, however due to time constraints (and a single
102 equipment failure), only the first 30 of the randomly selected sites were sampled during the study
103 (Table 1).

104

105 *Data collection*

106 To estimate overall abundance of rockfish on the Footprint Bank, we used a group of 7
107 stationary camera systems. The triggered camera (TrigCam) systems are described in Williams et
108 al. (2015, 2018), but were modified for the current project (Figure 2). In brief, the TrigCams are
109 a low-cost, still-image, stereo-camera system optimized for long duration deployments. These
110 cameras are capable of operating in “triggered” mode where images are only captured when
111 motion is detected in the view field. However, during this project, the cameras were configured
112 to collect a stereo-image pair every 30 seconds over the course of ~24 hour deployments.

113 The TrigCam consists of three housings (Figure 2). The main housing contains two
114 Chameleon3 USB 3 machine vision cameras, an ODroid-XU4-mini-ARM computer, and a
115 custom circuit board for power management and timing control of strobe pulses. The housing
116 was constructed from anodized aluminum with custom manufactured 80 mm radius acrylic
117 partial dome viewports for each camera. A second housing was manufactured from a 51 mm
118 thick acetal plastic plate and contained a neutral white-strobe unit powered by two TaskLED
119 Hyperboost strobe drivers. The system was powered by a 24 V 10 Ah nickel-metal hydride
120 battery pack housed in a cylindrical anodized aluminum housing. The three housings (cameras,
121 strobe, and batteries) were enclosed in a protective aluminum frame.

122 The TrigCams were deployed and retrieved using an acoustic release system
123 manufactured by DesertStar Systems ARC-1XD. The acoustic-release is attached to a small float
124 and line and was triggered from the surface using a deck box, after which the float rose to the
125 surface allowing retrieval of the unit. Thus, the TrigCams were untethered from the research
126 vessel and maintained a minimal profile during deployment on the seafloor (Figure 2).

127

128 *Image analysis*

129 Each TrigCam unit was calibrated for stereo-analysis using a standard stereo-calibration
130 routine (Bouguet 2008) modified for marine underwater stereo-camera systems by Williams et
131 al. (2010). Stereo-image analysis was performed using an open-source, stereo-processing
132 package (SEBASTES; Williams et. al, 2016). SEBASTES was used to identify fish to species
133 and estimate fish range and 3D position relative to the camera. Fish locations were estimated by
134 identifying a single corresponding point on each fish seen in both images, such as the fish eye.
135 Fish only partially visible in both image frames were only included when bordering the left and

136 upper sides of the images. In this way, these partial targets were assumed to be 50 % retained for
137 further analysis, reducing the possibility of under- or over-estimates of fish density. Individuals
138 from seven species of common rockfish and lingcod were counted in each frame of each
139 deployment (Table 2). The substrate observed in the underwater camera deployments was
140 classified by a commonly used seafloor substratum classification scheme (Stein et al. 1992;
141 Yoklavich et al. 2000) that consists of a two-letter coding of substratum type denoting a primary
142 substratum with > 50% coverage of the seafloor and a secondary substratum with 20% –49%
143 coverage of the seafloor. There were seven identified substratum types: mud (M), sand (S),
144 gravel-pebble (G, diameter < 6.5 cm), cobble (C, 6.5 < diameter < 25.5 cm), boulder (B,
145 diameter > 25.5 cm), exposed low-relief bedrock (R), and exposed high-relief bedrock (K).
146 Using this classification, a section of seafloor covered primarily in cobble, but with boulders
147 over more than 20% of the surface, would receive the substratum code cobble-boulder (Cb) with
148 the secondary substratum indicated by the lower-case letter. Since the underwater camera
149 deployments were stationary, the substrate classification was constant within each deployment.

150 To compute fish volumetric density, the volume imaged by both cameras was estimated
151 using a general approximation approach based on a point cloud (Williams et al. 2018). In brief,
152 stereo-image analysis relies on a set of equations that transform pixel coordinates of objects seen
153 by both cameras into real world coordinates using stereo-triangulation. The reverse
154 transformation is termed projection, resulting in the expected position of a real world object on
155 the camera image plane. We use the latter process to estimate the set of points from a generated
156 3D point cloud that occupy the joint stereo-camera image volume. This process therefore
157 accounts for the intrinsic camera calibration factors (e.g. lens distortion), and extrinsic factors
158 (the inter-camera geometry). To estimate joint image volume, a 3-dimensional grid of points at

159 10 cm separation was generated extending from the camera origin to a range of 9 m, with the
160 horizontal and vertical extent of the point cloud set to capture the entire view field. The points
161 were then projected back to pixel coordinate space, and only the points that constitute valid pixel
162 coordinates in both left and right camera images were retained (i.e. points that are located below
163 the seafloor are excluded). The grid points were subset into 0.5 m range bins from the camera,
164 and the volume of each range bin was then estimated by scaling the number of points contained
165 in the joint stereo-view and within range intervals by the volume they represent, which in this
166 analysis was 1 L or 0.001 m³. The volume of each frame that is below the seafloor was also
167 removed from the calculated volume according to the methods of Williams et al. (2018).

168 The imaging volume analysis provided estimates of above-seafloor volumes at range
169 intervals for each image frame in the dataset. To estimate fish density, fish counts for targets
170 found within a range interval were divided by the corresponding volume. Densities were then
171 aggregated by species and camera unit. In principle, fish density is expected to decline as the
172 ability to detect and identify fish becomes reduced with increasing target range from the camera.
173 To arrive at an unbiased estimate of density, the expected decline in detectability as a function of
174 range was modeled. A logistic function was used, defined as

$$175 \quad rd_r = \frac{L}{1+e^{-k(r-x_0)}} \quad , \quad (\text{eq. 1})$$

176 where rd is the relative density scaled to a maximum of one at range r from the camera, and L , k
177 and x_0 are the function parameters. Parameters were estimated by minimizing the negative log-
178 likelihood between the observed density at a site and range interval and the modeled density
179 assuming a normal error distribution. The deviations between observed and predicted density
180 were weighted by the respective volume of each range interval, so that the very small volumes
181 closest to the camera had less influence on the model than larger volume bins farther away. In

182 addition, the x_o parameter, which indicates the midpoint of the function curve, was restricted to
183 be greater than 2 m to prevent outcomes where density occasionally becomes exponentially
184 reduced from the first range interval onward by the presence of a single fish close to the camera.
185 Density for a species, d , for each frame, f , are then calculated as the sum of the species density at
186 each range, r , corrected for the detectability at that range, so that

$$187 \quad d_f = \sum_{i=1}^r \frac{d_{fr}}{rd_r} \quad (\text{eq. 2}).$$

188 The density of a species for a deployment (\bar{d}) was then calculated as the mean of d_f for that
189 deployment. All modeling and statistical analyses were done in R software (R Core Development
190 Team 2018) and R code for estimating the relative density function with documentation can be
191 downloaded as a package at <https://github.com/rooperc4/TrigCamDensityEstimation>.

192

193 *Data Analysis*

194 Densities were calculated for each frame of each deployment based on the volume of
195 water observed and the species-specific detection model described above. Densities by frame
196 were used to generate presences or absences for use as replicates for analyses of “within
197 deployment” processes. The mean density for deployments were then used as the replicates in
198 analysis of processes at the “deployment scale” and to estimate the population size for each
199 species of fish. In some analyses, deployments were split into daytime and nighttime segments to
200 facilitate comparisons.

201 To determine the effect of tidal cycles and diurnal cycles on the presence of fish, we used
202 a generalized additive mixed model (GAMM, Wood 2006) to test for significant linear or non-
203 linear effects of hour-of-the-day and hourly tidal change. This analysis used presence or absences
204 averaged over one hour intervals for each deployment as replicates. Aggregation of data to one

205 hour intervals helped to reduce autocorrelation in the data set. In preliminary analyses the raw
206 frame by frame data and aggregation over five, ten, and fifteen minute intervals were also tested.
207 None of these groupings had an effect on the shape of the relationships between variables and the
208 presence or absence of fish or on the significance of the relationships, but they did affect the
209 overall variance and the temporal aggregation (both increased with decreasing aggregation). The
210 tidal change was calculated from tide station harmonics using the nearest tide gauge (located in
211 Santa Barbara, CA) and was the difference in tidal height from one image frame to the next
212 (every 30 seconds) and averaged over one hour intervals. The tidal heights were estimated using
213 the rtide package in R software (Thorley et al. 2018). The GAMM was implemented with a
214 maximum of $k = 5$ knots to minimize overfitting and parametric (factor) terms were included for
215 species to account for species -specific differences in density. Deployment was treated as a
216 random effect, so that

$$217 \quad y = \alpha + s(\textit{tidal change}) + s(\textit{hour}) + \textit{species} + \textit{deployment} + \varepsilon \quad (\text{eq. 3})$$

218 Where y is presence or absence of fish, s indicates a thin-plate regression spline smoothing
219 function for the tidal change term and a cyclic cubic spline smoothing function for the hour term
220 (Wood 2006), α is an intercept and ε are binomial distributed errors. An autocorrelation term
221 nested within the deployment at lag = 1 was also included in the model.

222 Within-deployment variability was examined graphically to determine when the density
223 and variability in density peaked, and specifically if any “settling” period could be detected after
224 the initial TrigCam deployment where fish might have been scared from the area by the
225 approaching gear (data from a pilot study in the same area in 2016 were also used to address this
226 question and are reported in supplemental material).

227 The effect of substrate type on density was also tested but data for the analysis was
228 limited to imagery captured during daylight hours because of the small sample size of fishes
229 observed during nighttime hours and the results of GAMM modeling which indicated nighttime
230 and daytime data should not be combined for this analysis. An analysis-of-variance was used
231 with the density estimated for each deployment as replicates. Separate tests were conducted for
232 significant effect of primary substrate type and the significant effect of the presence of rocky
233 substrate (high and low relief bedrock or boulders) in either the primary or secondary substrate
234 classes. The effect of depth was also tested, with station depth separated into three depth strata:
235 90-110 m, 110-130 m and 130-150 m. Fish species was included as an effect in the analysis,
236 along with a primary substrate-species effect or a presence of rocky substrate-species effect, to
237 determine whether some species of fish were more abundant in some substrate types than others.
238 Tukey's post-hoc tests were used to examine significant effects in the analysis and significance
239 of all statistical tests was identified at $p < 0.05$.

240 Finally, a population abundance (and variance) for each species was calculated for the
241 entirety of Footprint Bank. For this estimate, the area of the bank at depths < 150 m (roughly the
242 area sampled during our study) was calculated as 0.682 km^2 from previous multibeam mapping
243 (Dartnell et al. 2005). This was expanded to 0.852 km^3 using the height of the water column
244 observed by the cameras (1.25 m). This estimate was then used to expand the volumetric
245 densities to a total abundance. Based on the results of the data analyses, three divisions of data
246 and two methods were used to calculate abundances. Non-stratified, random sampling formulae
247 were used to estimate abundances for all the data combined. Separate daytime and nighttime
248 abundances were also estimated. A second method that stratified the data by the substrate using
249 only daytime data was also used. Previous research by Yoklavich et al. (2011) indicated that

250 roughly 22.5% of the upper portion of Footprint Bank (< 200 m) is comprised of primarily
 251 bedrock, 7.5% is comprised of primarily high relief boulders, 55% is comprised primarily of
 252 cobble habitat and the remaining 15% is comprised of low relief unconsolidated substrates (sand
 253 and mud). Thus, based on stratification by these four substrate types, the strata area for rocky
 254 substrate was 0.192 km³, boulder substrate was 0.064 km³, cobble was 0.469 km³ and sand was
 255 0.128 km³. For a stratified estimate of abundance the densities of rockfish from deployments
 256 with the corresponding primary substrate type were expanded according to the strata area. For
 257 example, all deployments with a primary substrate of sand (n = 17) were expanded over the
 258 unconsolidated strata area (0.128 km³)

259 Abundance estimates and variances (both stratified and non-stratified) were calculated
 260 using the standard formulae of Thompson (1992). For unstratified estimates, the population total
 261 in number of fish $\hat{\tau}$ is:

$$262 \quad \hat{\tau} = A\bar{d} \quad (\text{eq. 4})$$

263 with variance

$$264 \quad \text{var}(\hat{\tau}) = A^2 \frac{s^2}{n} \quad (\text{eq. 5})$$

265 where N is the total study area, \bar{d} is the mean volumetric density, s^2 is the variance of the mean
 266 and n is the number of deployments. For stratified estimates of the population total, $\hat{\tau}_{st}$, the total
 267 population is the sum of the abundance in each strata h :

$$268 \quad \hat{\tau}_{st} = \sum_{h=1}^L A_h \bar{d}_h \quad (\text{eq.6})$$

269

270 with variance as the sum of each strata h variance is:

$$271 \quad \text{var}(\hat{\tau}_{st}) = \sum_{h=1}^L A_h^2 \frac{s_h^2}{n_h} \quad (\text{eq. 7})$$

272 where A_h is the strata area, \bar{d}_h is the mean volumetric density, s_h^2 is the variance of the mean and
273 n_h is the number of deployments in stratum h . Coefficients of variation were calculated as the
274 square-root of the variance divided by the abundance estimate. Since the sample size relative to
275 the total available samples was very small, the finite population correction was ignored.

276

277 **Results**

278

279 The detection function for each species indicated that most individuals were identifiable
280 out to about 2-4 m from the camera (Figure 3). Speckled rockfish and greenstriped rockfish
281 (*Sebastes elongatus*) were the exceptions, with speckled rockfish being difficult to identify and
282 count beyond 2.5 m and greenstriped rockfish easily identifiable at a range of over 5 m. The
283 model parameter x_0 for speckled rockfish was estimated at the minimum possible value (2 m).
284 Alternatively, this may indicate that they may have been attracted to the camera and thus
285 occurred within a nearer distance. However, all image analysts noted the difficulty in identifying
286 this species at far distances. The application of the detection function for each species resulted in
287 densities of fish ranging from 0 – 3.5 fish m^{-3} for individual frames. Observations were zero-
288 inflated, with 95.5% of 616,104 frames containing no sightings of the species of interest.

289 Generalized additive model results show that there was a significant diel effect on the
290 presence of rockfishes and lingcod ($p < 0.0001$). Rockfish probability of presence peaked around
291 mid-day and was lowest during nighttime (Figure 4). The effect of tidal change was also
292 significant ($p = 0.03$) with the probability of fish presence elevated at moderately rising and
293 falling tides (Figure 4). Species was also significant in the GAMM. The patterns of individual
294 species density during day and night hours indicated strong trends towards higher observed

295 densities during daylight hours for most species (Figure 5). The only species that appeared to
296 have higher densities during nighttime hours than daytime hours were bank rockfish (*S. rufus*)
297 and greenstriped rockfish.

298 The day-night differences in density of fishes had a strong influence on other facets of the
299 data. Since most deployments were started in the evening after dusk (Table 1), the variability in
300 density at a single site was minimal through the first few hours of the deployment (Figure 6).
301 With the onset of daylight, the variability in density at an individual site increased to a peak in
302 mid-afternoon (12:00 – 15:00) and then declined to low levels of variability in the evening. This
303 pattern was linked to changes in average density, as the standard deviation of density increased
304 linearly with increasing density (Figure 6).

305 It was impossible to determine the amount of time needed for rockfish densities to
306 stabilize after the effect of the deployment of the TrigCams for the 2017 deployments. This was
307 because the time of first arrival for fishes was strongly influenced by the timing of the
308 deployments (Figure 7). The elapsed time between deployment and appearance of the first fish
309 was highly variable across species, but only bocaccio rockfish (*S. paucispinis*) and greenspotted
310 rockfish (*S. chlorostictus*) had median first arrival times prior to dawn. During a pilot study in
311 2016, it was found that for daytime deployments, the average elapsed time between deployment
312 and the arrival of the first rockfish was 87 minutes (SD = 78, see S1 for details on this analysis).

313 The same density estimates could be generated from two types of behavior. A single
314 stationary fish observed in 50 consecutive frames of a deployment could generate the same
315 density as 50 fish observed in a single frame during the deployment. For example, lingcod were
316 often seen in consecutive frames (the maximum during one deployment was 24), whereas
317 bocaccio rockfish tended to show greater mobility, with the maximum consecutive frames in

318 which a fish was observed being five during a single deployment. Both of these deployments
319 produced close to the same density estimate(Figure 8). In fact, with the exception of speckled
320 rockfish, the density of fishes was unrelated to the maximum number of frames in which fish
321 were consecutively observed. This indicates that the same range of densities ($0 - 0.3 \text{ fish} * \text{m}^{-3}$)
322 were being produced by both fish that were moving around and those that were stationary and
323 repeatedly observed.

324 Primary substrate type also had a significant effect on fish density in the Footprint Bank
325 area (Table 3). Tukey's post-hoc tests indicated that the primary substrate types of bedrock (high
326 and low relief) had significantly higher densities than other types of primary substrates. There
327 were no significant differences found among the other substrates. A species-primary substrate
328 interaction term was highly significant in the analysis as well ($p < 0.0001$), although post-hoc
329 tests revealed that the significant differences were related to high densities to greater densities of
330 speckled rockfish (5x) at sites with bedrock as the primary substrate than all other fish-habitat
331 combinations (Figure 9). There were no significant differences among other species-primary
332 substrate combinations. Site depth was also not significant in the analysis, indicating a minimal
333 effect of depth (at least across the limited range of 90 - 150 m explored here). When the presence
334 of rocky substrate was included as an explanatory variable in the ANOVA in the place of
335 primary substrate type, only species was significant ($p = 0.002$). Depth, the presence of rocky
336 substrate, and the interaction between presence of rocky substrate and species were all
337 insignificant ($p > 0.05$).

338 Based on these results, abundance estimates were computed for each species using the
339 TrigCam deployments as replicates for 1) all data combined, 2) daytime only, 3) nighttime only
340 and 4) daytime only and stratified by primary substrate type. The resulting estimates were highly

341 variable both within and across species (Figure 10). Stratified estimates of the daytime data
342 tended to give the highest estimates of abundance for all species with the lowest average
343 coefficient of variation (CV = 0.57). The CV for these stratified estimates ranged from 0.23 for
344 bocaccio rockfish to 0.96 for lingcod. Using only nighttime data resulted in the lowest abundance
345 estimates for all species (except bank rockfish) and the highest average coefficient of variation
346 (CV = 0.81), ranging from 0.43 for greenspotted rockfish to 1.00 for flag rockfish (*S.*
347 *rubrivinctus*) and cowcod. (*S. levis*). Using unstratified daytime-only data and using all the data
348 from both day and night gave estimates of the average coefficient of variation of 0.59 and 0.63
349 across all species respectively. For individual species the average values of CV ranged from 0.23
350 (greenspotted rockfish) to 0.96 (lingcod) for daytime estimates and ranged from 0.22 for
351 (greenspotted rockfish) to 0.96 (lingcod) for all data. The most abundant species was speckled
352 rockfish with a population of 12,994 individuals (SE = 6,722) within the surveyed area of
353 Footprint Bank (stratified estimate). Greenstriped rockfish were estimated to be the least
354 abundant with an estimate of only 82 individuals (SE = 50) within the surveyed area of Footprint
355 Bank.

356

357 **Discussion**

358

359 Population estimates of rockfish that included a habitat stratification showed a marginal
360 improvement in precision (i.e. CV) for bocaccio rockfish, cowcod, bank rockfish and speckled
361 rockfish compared to a random survey design. This was not surprising given the known affinity
362 of rockfish for highly rugose habitats (Love et al. 1991, Jones et al. 2012, Yoklavich 2013).
363 However, the improvement of CV with stratification for these species was relatively small

364 (~7%). There was an increase in the estimate of abundance for all species when stratification by
365 primary substrate type was used. Sand was the primary substrate at 17 of the 30 deployment sites
366 (Table 1). Although the abundance from the 13 deployments in the rocky strata was higher than
367 for the sand strata, the increased in variability with increased density negated most of the
368 improvement in precision that could be gained by stratification. A more efficient sample
369 allocation scheme could have improved the results and given more precise estimates of
370 abundance by placing a higher number of samples within the high density-high variability rocky
371 strata for some species. In the current study, more samples (17) were allocated to sand habitat
372 stratum where density was lower than the rocky habitat strata (bedrock = 4, boulder = 5 and
373 cobble = 4). To maximize the precision of estimates of rockfish a Neyman allocation (Thompson
374 1992) incorporating the observed strata variances (averaged across species) from this study
375 would allocate 70.0% of stations into the bedrock stratum, 5.2% of stations into the boulder
376 stratum, 19.3% of stations into the cobble stratum and 5.5% of stations into the sand strata. For
377 individual species this allocation scheme varied depending on their variances among strata.
378 Bocaccio rockfish for example, which had a relatively low CV for the stratified population
379 estimate (23%), were relatively close to the optimal station allocation.

380 The results of this study showed that environmental factors can significantly influence the
381 measured density and encounter rates of rockfishes. Diurnal cycles in particular had a large
382 influence on the probability of presence and perceived density of rockfish during the study,
383 whereas tidal cycles while significant did not appear to affect rockfish as much. Substrate type
384 was also an important factor in determining density of rockfish and this effect varied among
385 species, highlighting the likely importance of stratification in producing abundance estimates.
386 The overall goal of this study was to produce population (and variance) estimates for Footprint

387 Bank using stationary cameras as an alternative sampling method. There are some important
388 differences in terms of the area surveyed between these stationary cameras and more traditional
389 survey methods for rockfish such as bottom trawls and more recently developed mobile camera
390 systems (remote-operated vehicles, manned submersibles and autonomous underwater vehicles).
391 The average field-of-view (FOV) for the stationary cameras during each deployment was 27.8
392 m³ (SE = 0.45), while bottom trawl surveys typically cover > 1 ha (10,000 m²) of seafloor and
393 mobile camera surveys typically cover 500 - 1000 m² of seafloor in each deployment (Yoklavich
394 et al. 2007, Tolimieri et al. 2008, Clarke et al. 2009, Rooper et al. 2016, Stierhoff et al. 2016).
395 Despite the large differences in spatial coverage obtained between methods, the abundance
396 estimates from the stationary camera survey of Footprint Bank were comparable to previous
397 studies conducted in 2011 and 2009 using manned submersibles and remotely operated vehicles
398 (Stierhoff et al. 2013, Yoklavich et al. 2013). The TrigCam estimates of abundance tended to be
399 lower than the other two surveys for Footprint Bank (Figure 11), with the exception of speckled
400 rockfish and greenspotted rockfish (the two most common species in the TrigCam survey). The
401 deployment depths (Table 1) and total area sampled by the TrigCam survey was slightly less
402 than for the other two surveys which may partially explain the observed differences. The
403 coefficients of variation of the estimates of abundance were similar across three studies, although
404 both the ROV and TrigCam surveys showed a wider range of CV's across the shared species
405 than the manned submersible.

406 One of the major implications for assessing rockfishes from this study is that the time of
407 day during which the survey is conducted is important to perceived densities of fishes. Fish
408 abundance at stationary cameras was higher during daylight hours when fish were more likely to
409 be active and moving throughout the area. However, this effect was species-specific, with bank

410 rockfish and greenstriped rockfish more likely to be observed during nighttime hours. This is
411 consistent with other research that has found diel behaviors are important for rockfishes (Stanley
412 et al. 1999, Stanley et al. 2000, Ressler et al. 2009, Rooper et al. 2010). In a study of rocky
413 habitat in the eastern Bering Sea, northern rockfish (*S. polyspinis*) were observed to rise into the
414 water column to feed during daylight hours and settle to the seafloor at night; whereas juvenile
415 Pacific ocean perch (*S. alutus*) were more likely to be observed in higher densities near the
416 seafloor during daylight hours (Rooper et al. 2010). Stanley et al. (2000, 2007) and Ressler et al.
417 (2009) both observed schooling rockfishes in the water column during nighttime hours. This
418 behavior has been linked to feeding patterns, which is also consistent with the information
419 available for greenstriped rockfish which tend to feed on fishes, shrimps and squids which may
420 be more available near the seafloor at night, in addition to zooplankton (Love et al. 2002).
421 Identifying the diel behavior of the species to be assessed is important in interpreting perceived
422 abundance, especially where survey gear can only observe a limited part of the animal's habitat,
423 such only near the seafloor for benthic camera systems or only in the water column for acoustic
424 systems (Rooper et al. 2010). In addition this has major implications for survey design and
425 execution regardless of using an optical or more traditional fisheries gear, such as a bottom trawl.

426 One objective of this study was to identify the length of time fish needed to acclimate to
427 the presence of the TrigCam. However, we found no detectible difference in times of arrival to
428 the stationary cameras that would indicate fish left the area during deployment and returned. This
429 may indicate that there was no acclimation time necessary after the deployment of the camera,
430 however, there are a number of other potential explanations. The lack of observed effect may
431 have been the result of the interval length (30 seconds) between captured images being long
432 enough that fish reactions occurred prior to capturing the initial image. The lack of effect was

433 more likely a result of the relative paucity of rockfish observed during nighttime hours when
434 most cameras were deployed. During the night, most species were either less active or less
435 abundant in the study area, so unless the camera was deployed near a fish, it was likely that no
436 reaction would have been observable. There was no indication from the data that there was a
437 difference in fish behavior in response to the camera deployment between night and day. For
438 example, we did not observe any marked orientation behavior to the camera, and fish were
439 observed both arriving and departing from the FOV. The relative unobtrusiveness of the
440 TrigCam compared to other survey gears, especially mobile gears (e.g. manned submersibles or
441 remote operated vehicles), may have contributed to the absence of a perceived response to
442 deployment of the cameras.

443

444 **Conclusion**

445 This study showed the importance of considering the behavior of target species and its
446 interaction with perceived density when designing a survey to estimate fish abundance.
447 Underwater camera surveys have parallel issues to traditional survey methods such as bottom
448 trawls and longlines in terms of fish availability by habitat and fish detectability by the gear. For
449 camera surveys, these issues are often related to the behavior of the fishes. Thus, it is important
450 to continue to study and estimate the effects of survey equipment on fish behavior and perceived
451 abundance. In this study, stratification of the survey area by habitat type had an effect on the
452 estimates of population size and a limited impact on the variance estimate. This indicates that
453 optimizing the allocation of samples and simulation of optimal allocation schemes is likely to
454 point to directions that can further improve abundance estimation for rockfishes in untrawlable
455 habitats.

456

457 **Acknowledgements**

458

459 We thank Dave Somerton, Matt Campbell, Mary Yoklavich, Liz Clarke, Waldo
460 Wakefield, Tom Laidig, Diane Watters, Erica Fruh, Curt Whitmire, Jennifer Boldt, Vanessa
461 Tuttle, Jodi Pirtle, Jeff Anderson, the RV *Shearwater*, and the FSV *Bell M. Shimada* for their
462 assistance in conducting the fieldwork and for their discussions of concepts and drafts of this
463 manuscript. We are grateful for David Somerton's initial invitation to join the NMFS
464 Untrawlable Strategic Initiative and his encouragement during the project. The study was funded
465 by Rick Methot through NOAA Fisheries Office of Science and Technology's Untrawlable
466 Habitat Strategic Initiative. Helpful manuscript reviews were provided by Matt Campbell, David
467 Bryan, Jeff Napp, Wayne Palsson, Stan Kotwicki and two anonymous reviewers.

468 The findings and conclusions in the paper are those of the authors and do not necessarily
469 represent the views of the National Marine Fishery Service, NOAA. Reference to trade names
470 does not imply endorsement by the National Marine Fisheries Service, NOAA.

471

472 **References**

473

474 Bacheiler, N.M., Schobernd, C.M., Schobernd, Z.H., Mitchell, W.A., Berrane, D.J., Kellison,
475 G.T., and Reichert, M.J.M. 2013. Comparison of trap and underwater video gears for
476 indexing reef fish presence and abundance in the southeast United States. *Fish. Res.*
477 143:81-88.

478 Bacheiler, N.M., Berrane, D.J., Mitchell, W.A., Schobernd, C.M., Schobernd, Z.H., Teer, B.Z.,
479 and Ballenger, J.C. 2014. Environmental conditions and habitat characteristics influence

480 trap and video de-tecton probabilities for reef fish species. *Marine Ecology Progress*
481 *Series*, 517:1–14. <https://doi.org/10.3354/meps11094>

482 Bachelier, N.M., and Shertzer, K.W. 2015. Estimating relative abundance and species richness
483 from video surveys of reef fishes. *Fish. Bull.* 113:15-26.

484 Bouguet, J.Y. 2008. Camera Calibration Toolbox for Matlab [online]. Available from
485 vision.caltech.edu/bouguetj/calib_doc/index.html [accessed 20 September 2008].

486 Bryan, D.R., Bosley, K.L., Hicks, A.C., Haltuch, M.A. and Wakefield, W.W. 2014. Quantitative
487 video analysis of flatfish herding behavior and impact on effective area swept of a survey
488 trawl. *Fish. Res.* 154: 120-126.

489 Bublitz, C.G. 1996. Quantitative evaluation of fish behaviour during capture by trawl gear. *Fish.*
490 *Res.* 25: 293–304.

491 Campbell, M.D., Pollack, A.G., Gledhill, C.T., Switzer, T.S., and DeVries, D.A. 2015.
492 Comparison of relative abundance indices calculated from two methods of generating
493 video count data. *Fish. Res.* 170:125-133.

494 Clarke, M.E., Tolimieri, N., and Singh, H. 2009. Using the seabed AUV to assess populations of
495 groundfish in untrawlable areas, p. 357-372.. In: Beamish R.J., Rothschild B.J. (eds), *The*
496 *Future of Fisheries Science in North America*. Fish & Fisheries Series, vol 31. Springer,
497 Dordrecht

498 Cordue, P. 2007. A note on non-random error structure in trawl survey abundance indices.
499 *ICES J. Mar. Sci.* 64:1333-1337.

500 Dartnell, P., Cochrane, G., and Dunaway, M.E. 2005. Multibeam bathymetry and backscatter
501 data: Northeastern Channel Islands region, Southern California, U.S. Geological Survey
502 Open-File Report 05-1153, <http://pubs.usgs.gov/of/2005/1153/>.

503 DeRobertis, A., Taylor, K., Williams, K., and Wilson, C.D. 2017. Species and size selectivity of
504 two midwater trawls used in acoustic survey of the Alaska arctic. *Deep-Sea Res. II*.
505 135:40-50.

506 Geraldi, N.R., Bacheler, N.M, and Kellison, G.T. 2019. Method-dependent influence of
507 environmental variables on reef fish assemblages when comparing trap and video
508 surveys. *Mar. Ecol.* 40:e12538. <https://doi.org/10.1111/maec.12538>

509 Huse, I., Lokkeborg, S., and Soldal, A.V. 2000. Relative selectivity in trawl, longline, and gillnet
510 fisheries for cod and haddock. *ICES J. Mar. Sci.* 57:1271-1282.

511 Jones, D.T., Wilson, C.D., De Robertis, A., Rooper, C.N., Weber, T.C., and Butler, J.L. 2012.
512 Evaluation of rockfish abundance in untrawlable habitat: combining acoustic and
513 complementary sampling tools. *Fish. Bull. U,S*, 110:332-343.

514 Kilfoil, J.P. Wirsing, A.J., Campbell, M.D., Kiszka, J.J., Gastrich, K.R., Heithaus, M.R., Zhang,
515 Y., and Bond, M.E. 2017. Baited remote underwater video surveys undercount sharks at
516 high densities: insights from full-spherical camera technologies. *Mar. Ecol. Prog. Ser.*
517 585:113-121.

518 Kotwicky, S., De Robertis, A., von Szalay, P., and Towler, R. 2009. The effect of light intensity
519 on the availability of walleye pollock (*Theragra chalcogramma*) to bottom trawl and
520 acoustic surveys. *Can. J. Fish. Aquat. Sci.* 66:983-994.

521 Laidig, T.E., Krigsman, L.M., and Yoklavich, M.M. 2013. Reactions of fishes to two underwater
522 survey tools, a manned submersible and a remotely operated vehicle. *Fish. Bull., U.S.*
523 111(1): 54-67.

524 Lorance, P. and Trenkel, V.M. 2006. Variability in natural behavior, and observed reactions to
525 an ROV, by mid-slope fish species. *J. Exp. Marine Biol. Ecol.* 332:106-119.

526 Love M.S., Yoklavich, M., and Thorsteinson, L. 2002. The Rockfishes of the Northeast Pacific.
527 University of California Press, Berkeley and Los Angeles California.

528 Love, M.S., Carr, M.H., and Haldorson, L.J. 1991. The ecology of substrate-associated juveniles
529 of the genus *Sebastes*. *Environ. Biol. Fish.* 30: 225–243.
530 <http://dx.doi.org/10.1007/BF02296891>

531 Mallet, D. and Pelletier, D. 2014. Underwater video techniques for observing coastal marine
532 biodiversity: A review of sixty years of publications (1952-2012). *Fish. Res.* 154:44-62.

533 Munro, P.T. and Somerton, D.A.. 2002. Estimating net efficiency of a survey trawl for flatfishes.
534 *Fish. Res.* 55:267-279.

535 R Core Development team. 2018 R: A language and environment for statistical computing. R
536 Foundation for Statistical Computing, Vienna, Austria. ISBN 3-900051-07-0, URL
537 <http://www.R-project.org>.

538 Ressler, P.H., Fleischer, G.W., Wespestad, V.G, and Harms, J. 2009. Developing a commercial-
539 vessel-based stock assessment survey methodology for monitoring the U.S. West Coast
540 widow rockfish (*Sebastes entomelas*) stock. *Fish. Res.* 99:63-73.

541 Rooper C.N., Sigler, M., Goddard, P., Malecha, P.W., Towler, R., Williams, K., Wilborn, R., and
542 Zimmermann, M. 2016. Validation and improvement of species distribution models for
543 structure forming invertebrates in the eastern Bering Sea with an independent survey.
544 *Mar. Ecol. Prog. Ser.* 551:117-130.

545 Rooper, C.N., Hoff, G.R., and De Robertis, A. 2010. Assessing habitat utilization and rockfish
546 (*Sebastes* sp.) biomass in an isolated rocky ridge using acoustics and stereo image
547 analysis. *Can. J. Fish. Aquat. Sci.* 67:1658-1670.

548 Rooper, C.N., Martin, M.H., Butler, J.L., Jones, D.T., and Zimmermann, M. 2012. Estimating
549 species and size composition of rockfishes to verify targets in acoustic surveys of
550 untrawlable areas. *Fish. Bull.* 110:317-331.

551 Rooper, C.N., Williams, K., De Robertis, A., and Tuttle, V. 2015. Effect of underwater lighting
552 on observations of density and behavior of rockfish during camera transects. *Fish. Res.*
553 172:157-167.

554 Somerton, D.A., and Munro, P. 2001. Bridle efficiency of a survey trawl for flatfish. *Fish. Bull.*,
555 U.S. 99:641-652.

556 Somerton, D.A., Williams, K., and Campbell, M.D. 2017. Quantifying the behavior of fish in
557 response to moving camera vehicle by using benthic stereo cameras and target tracking.
558 *Fish. Bull.*, U.S. 115:343-354.

559 Stanley, R.D., Kieser, R., Leaman, B.M., and Cooke, K.D. 1999. Diel vertical migration by
560 yellowtail rockfish, *Sebastes flavidus*, and its impact on acoustic biomass estimation.
561 *Fish. Bull.*, U.S. 97:320-331.

562 Stanley, R.D., Kieser, R., Cooke, K., Surry, A.M., and Mose, B. 2000. Estimation of a widow
563 rockfish (*Sebastes entomelas*) shoal off British Columbia, Canada as a joint exercise
564 between stock assessment staff and the fishing industry. *ICES J. Mar. Sci.* 57:1035-1049.

565 Stein, D.L., Tissot, B.N., Hixon, M.A., and Barss, W. 1992. Fish-habitat associations on a deep
566 reef at the edge of the Oregon continental shelf. *Fish. Bull.*, U.S. 90: 540-551.

567 Stierhoff, K.L., Murfin, D.W., Demer, D.A., Mau, S.A., and Pinkard-Meier, D.R. 2016.
568 Improving the estimations of transect length and width for underwater visual surveys of
569 targets on or near the seabed. *ICES J. Mar. Sci.* 73:2729-2736.

570 Stierhoff, K.L., Butler, J.L., Mau, S.A., and Murfin, D.W. 2013. Abundance and biomass
571 estimates of demersal fishes at the Footprint and Piggy Bank from optical surveys using a
572 remotely operated vehicle (ROV). NOAA-TM-NMFS-SWFSC-521. US Department of
573 Commerce, Technical Memorandum, Southwest Fisheries Science Center, La Jolla, CA.

574 Stone, R.P., Masuda, M.M., and Karinen, J.F. 2015. Assessing the ecological importance of red
575 tree coral thickets in the eastern Gulf of Alaska. *ICES J. Mar. Sci.* 72:900-915.

576 Schroeder, D.M. and Love, M.S. 2002. Recreational fishing and marine fish populations in
577 California. *CalCOFI Rep* 43:182-190

578 Stoner, A.W., Ryer, C.H., Parker, S.J., Auster, P.J., and Wakefield, W.W. 2008. Evaluating the
579 role of fish behavior in surveys conducted with underwater vehicles. *Can. J. Fish. Aquat.*
580 *Sci.* 65:1230-1243.

581 Thompson, S.K. 1992. *Sampling*. John Wiley, New York, New York. 343 pp.

582 Thorley, J., Miller, L., and Fleishman, A. 2018. rtide: Tide Heights. R package version 0.0.5.
583 <https://github.com/poissonconsulting/rtide>

584 Tolimieri, N., Clarke, E.M., Singh, H., and Goldfinger, C. 2008. Evaluating the SeaBED AUV
585 for Monitoring Groundfish in Untrawlable Habitat, p. 99-107. In J.R. Reynolds and H.G.
586 Greene (editors), *Marine Habitat Mapping Technology for Alaska*. Alaska Sea Grant
587 College Program Rep. No. AK-SG-08-03, University of Alaska, Fairbanks.

588 Trenkel V.M., Lorange, P., and Mahévas, S. 2004. Do visual transects provide true population
589 density estimates for deepwater fish? *ICES J. Mar. Sci.* 61(7):1050-1056.

590 Trenkel V.M., Francis, R.I.C.C., Lorange, P., Mahévas, S., Rochet, M.J., and Tracey, D.M.
591 2004b. Availability of deep-water fish to trawling and visual observation from a remotely
592 operated vehicle (ROV). *Mar. Ecol. Prog. Ser.* 284:293-303. Weinberg, K. L. 2003.

593 Change in the performance of a Bering Sea survey trawl due to varied trawl speed.
594 Alaska Fish. Res. Bull. 10:42-49.

595 Weinberg, K.L. and Kotwicki, S. 2008. Factors influencing net width and sea floor contact of a
596 survey bottom trawl. Fish. Res. 93:265-279.

597 Williams, K., Punt, A.E., Wilson, C.D., and Horne, J.K. 2011. Length-selective retention of
598 walleye pollock, *Theragra chalcogramma*, by midwater trawls. ICES J. Mar. Sci.
599 68:119–129.

600 Williams, K., Horne, J.K., and Punt, A.E. 2015. Examining influences of environmental, trawl
601 gear, and fish population factors on midwater trawl performance using acoustic methods.
602 Fish. Res. 164:94–101.

603 Williams, K., De Robertis, A.W., Berkowitz, Z., Rooper, C.N., and Towler, R. 2015. An
604 underwater stereo-camera trap. Methods Oceanogr. 11:1-12.

605 Williams, K., Rooper, C.N., and Towler, R. 2010. Use of stereo camera systems for assessment
606 of rockfish abundance in untrawlable areas and for recording pollock behavior during
607 midwater trawls. Fish. Bull., U.S. 108:352-362.

608 Williams, K., Rooper, C.N., De Robertis, A., Levine, M., and Towler, R.H. 2018. A method for
609 computing volumetric fish density using stereo cameras. J Exp. Mar. Biol. Ecol. 508:21-
610 26.

611 Williams, K., Towler, R., Goddard, P., Wilborn, R., and Rooper, C. 2016. *Sebastes* stereo image
612 analysis software. AFSC Processed Rep. 2016-03, 42 p. Alaska Fish. Sci. Cent., NOAA,
613 Natl. Mar. Fish. Serv., 7600 Sand Point Way NE, Seattle WA 98115.

614 Wood, S.N. 2006. Generalized Additive Models: An Introduction with R. Chapman & Hall/CRC
615 Press, Boca Raton, FL.

616 Yoklavich, M., Laidig, T., Watters, D. and Love, M. 2013. Understanding the capabilities of new
617 technologies and methods to survey west coast groundfishes: Results from a visual
618 survey conducted in 2011 using the Dual Deepworker manned submersible at Footprint
619 and Piggy banks off southern California. Research Report available online at
620 <https://swfsc.noaa.gov/publications/CR/2013/2013Yoklavich.pdf>

621 Yoklavich, M.M., Greene, H.G., Cailliet, G.M., Sullivan, D.E., Lea, R.N., and Love, M.S. 2000.
622 Habitat associations of deep-water rockfishes in a submarine canyon: an example of a
623 natural refuge. Fish. Bull., U.S. 98:625-641.

624 Yoklavich, M.M., Love, M.S., and Forney, K.A., 2007. A fishery-independent assessment of an
625 overfished rockfish stock, cowcod (*Sebastes levis*), using direct observations from an
626 occupied submersible. Can. J. Fish. Aquat. Sci. 64:1795-1804.

627
628

629 **Tables**

630

631 Table 1. Characteristics of each TrigCam deployment on Footprint Bank in the southern
632 California Bight.

633

Deployment	Time of deployment	Depth of deployment	Primary substrate
1	10/12/17 20:12	101	Sand
2	10/12/17 19:47	105	Boulder
3	10/12/17 19:23	97	High Bedrock
4	10/12/17 18:58	141	Low Bedrock
5	10/13/17 19:08	133	Cobble
6	10/13/17 18:48	134	Cobble
7	10/13/17 20:15	100	Cobble
8	10/14/17 18:57	134	Boulder
9	10/14/17 20:22	134	Sand
10	10/14/17 19:58	117	Sand
11	10/16/17 4:44	141	Sand
12	10/16/17 4:16	116	Boulder
13	10/16/17 19:07	100	Sand
14	10/17/17 4:06	98	Boulder
15	10/17/17 4:42	117	Sand
16	10/17/17 5:04	121	Sand
17	10/18/17 4:02	113	Boulder
18	10/18/17 4:25	117	Sand
19	10/18/17 4:59	111	High Bedrock
20	10/19/17 4:05	101	Sand
21	10/19/17 4:24	120	Sand
22	10/19/17 4:49	121	Sand
23	10/21/17 17:38	105	Boulder
24	10/21/17 18:16	122	Sand
25	10/21/17 17:51	105	Sand
26	10/22/17 4:33	121	Sand
27	10/22/17 4:26	123	Cobble
28	10/23/17 4:04	112	Sand
29	10/23/17 4:34	115	Sand
30	10/23/17 4:48	105	Sand

634

635 Table 2. Species used in the analyses of rockfish abundance and density on 30 deployments from
 636 Footprint Bank in the southern California Bight.
 637

Common name	Species name	Number observed	Frequency of occurrence
Bank rockfish	<i>Sebastes rufus</i>	148	5
Cowcod	<i>S. levis</i>	90	9
Flag rockfish	<i>S. rubrivinctus</i>	54	7
Speckled rockfish	<i>S. ovalis</i>	660	20
Bocaccio	<i>S. paucispinnis</i>	302	22
Greenspotted rockfish	<i>S. chlorostictus</i>	2337	26
Greenstriped rockfish	<i>S. elongatus</i>	253	4
Lingcod	<i>Ophiodon elongatus</i>	178	3

638
 639
 640 Table 3. Analysis of variance table testing for differences in density among primary substrate
 641 types, species and depth bins.
 642

Variable	Df	Sum Sq	Mean Sq	F value	Pr(>F)
Primary substrate type	4	0.001714	0.000429	4.302	0.0023
Species	7	0.002840	0.000406	4.073	0.0003
Depth	2	0.000135	0.000068	0.680	0.5078
Primary substrate*Species	28	0.007233	0.000258	2.594	0.0001
Residuals	206	0.020516	0.000100		

643
 644
 645
 646

647 **Figures**

648
649
650
651
652
653
654
655
656
657
658
659
660
661
662
663
664
665
666
667
668
669
670
671
672
673
674
675
676
677
678
679
680
681
682

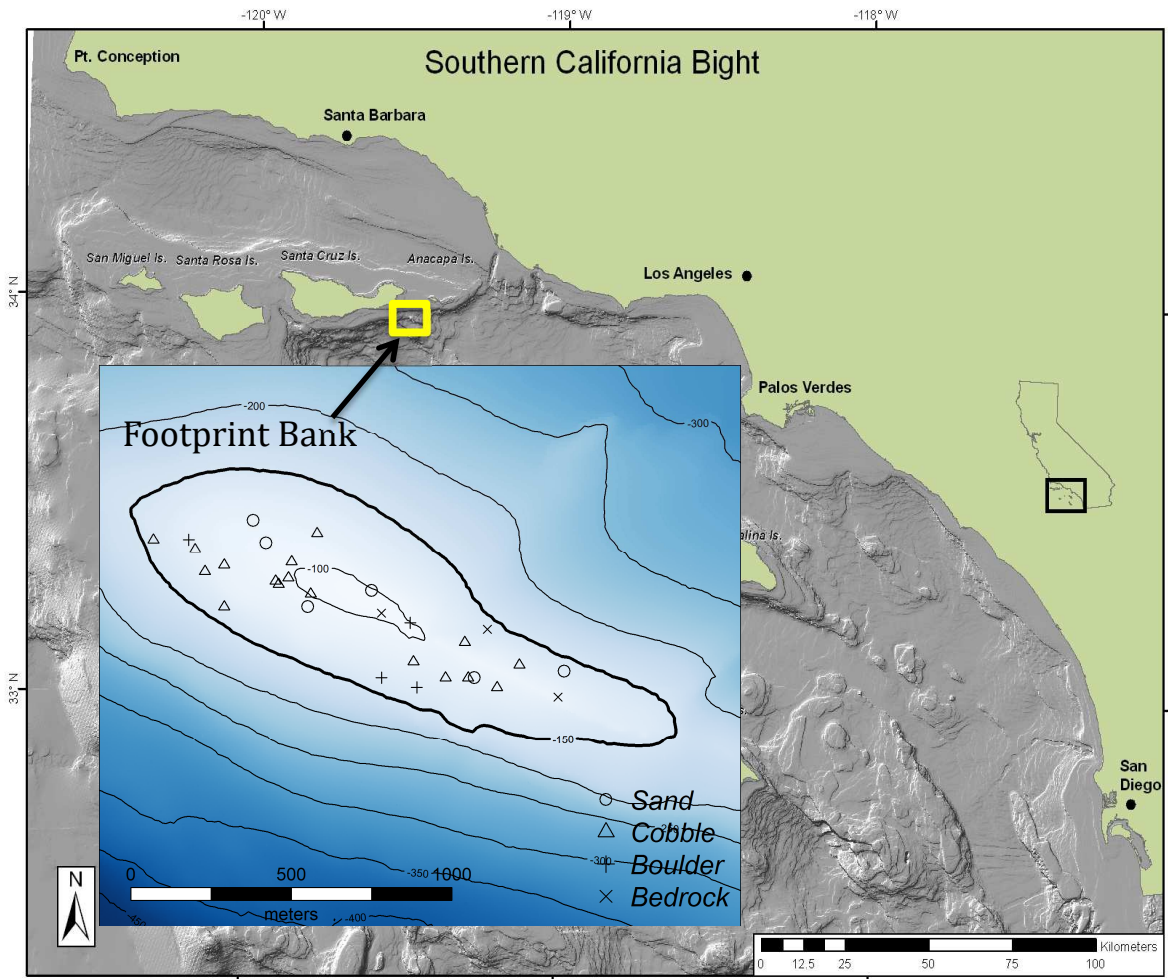
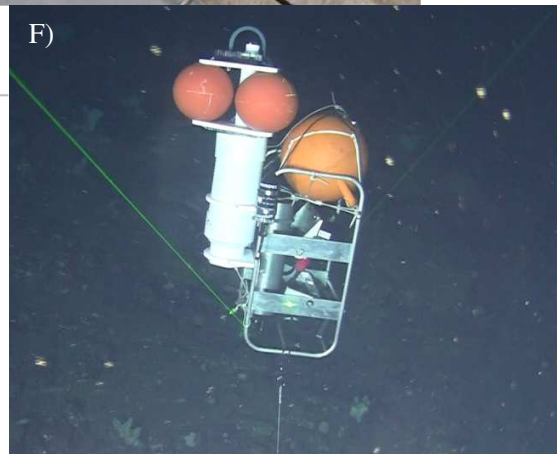
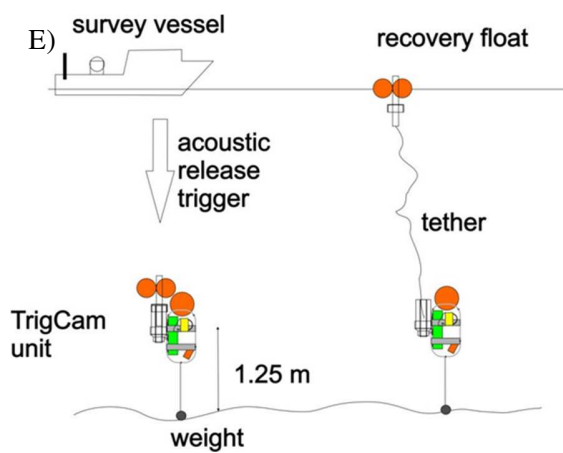


Figure 1. A map of Footprint Bank located in southern California south of Santa Cruz and Anacapa Islands. Dots indicate location of the 30 Triggcam deployments color coded by primary substrate type. The heavy contour line is the 150 m depth contour demarking the area of the study.



683



684

685

686

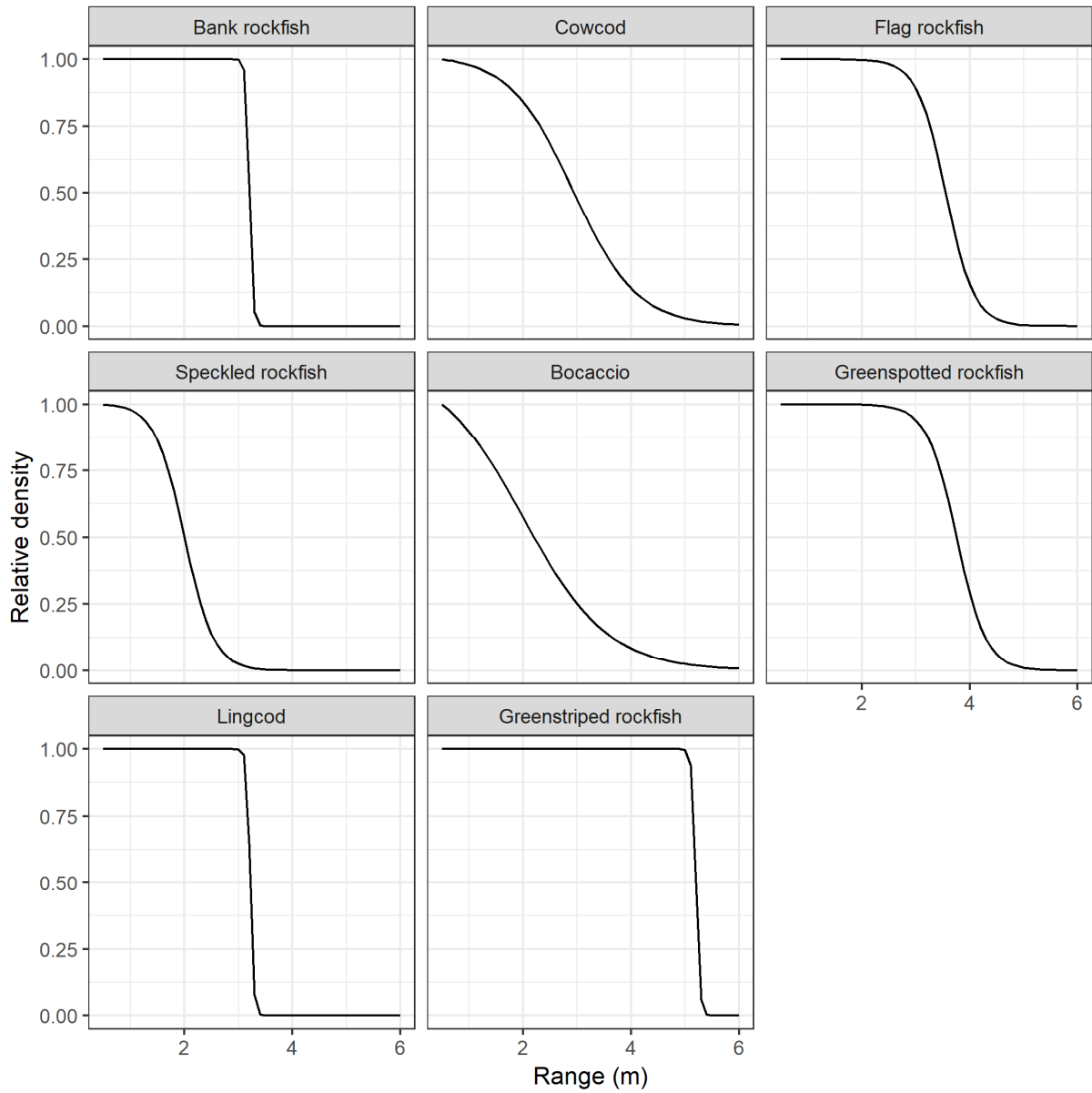
687

688

689

Figure 2. Image of TrigCam components (A-C), fully assembled TrigCam inside an aluminum frame (D), illustration of the deployment and recovery system (E), and deployed TrigCam (photo from manned submersible, F).

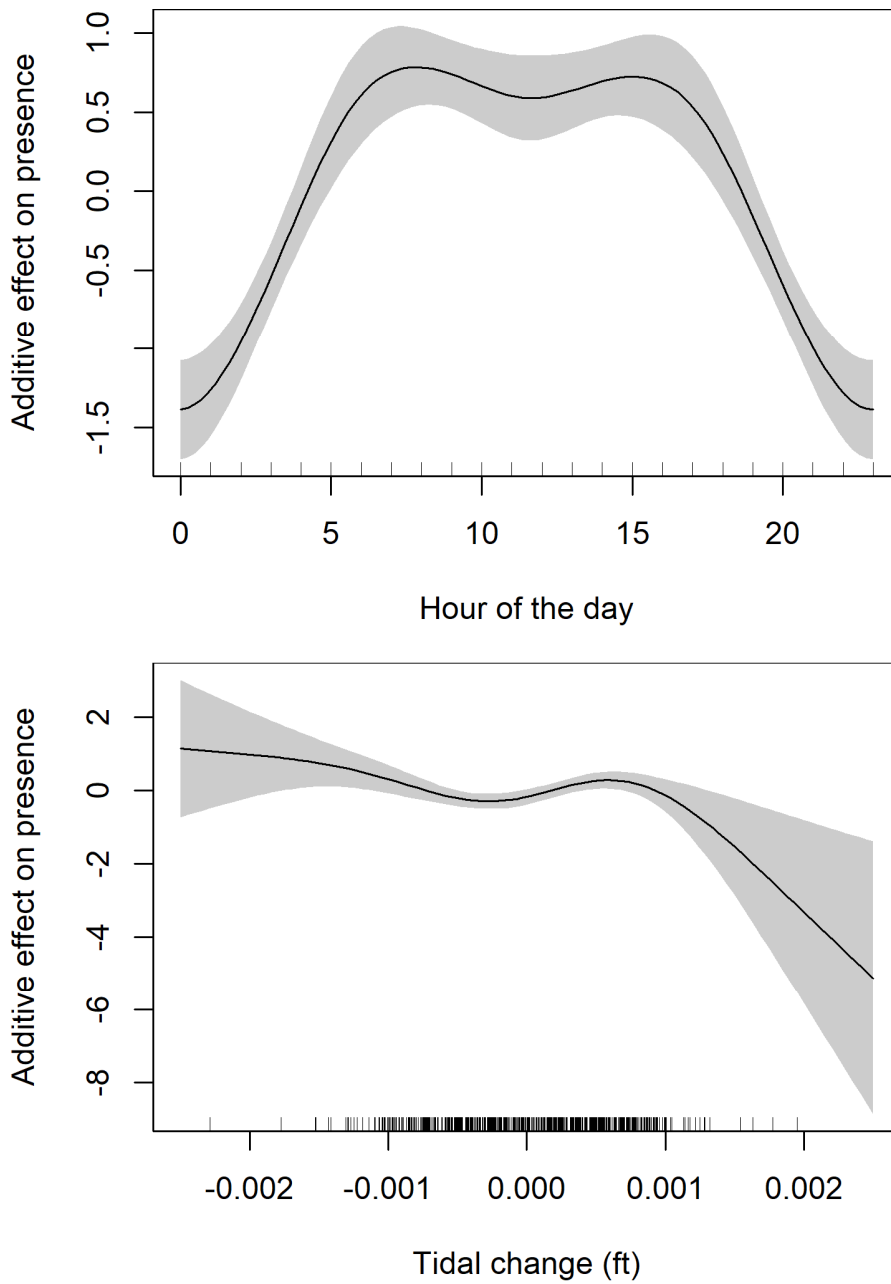
690



691
692
693
694
695
696

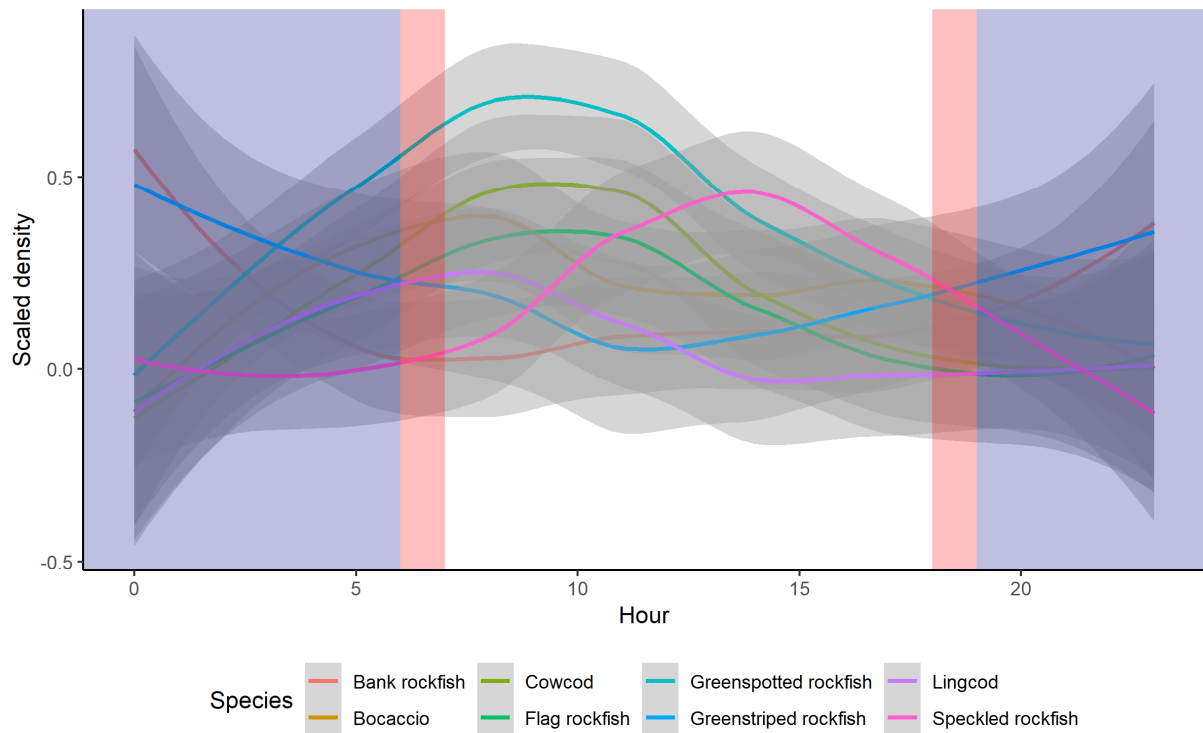
Figure 3. Detection function for rockfish species portraying the relative density of each species (scaled to 1) as a function of distance (range) from the stationary camera platform (m).

A)



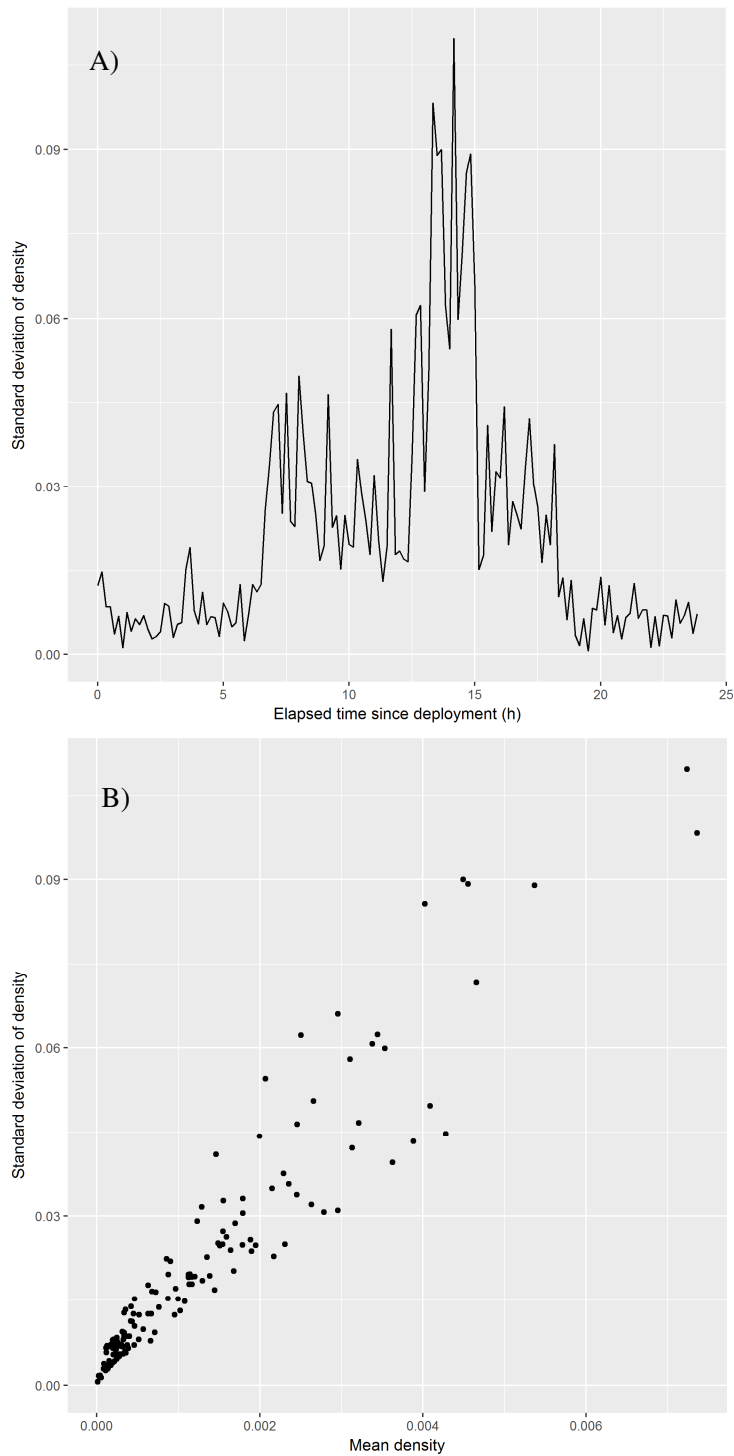
697
 698
 699
 700
 701
 702
 703

Fig. 4. Relationships from a generalized additive model of the effect of the hour of the day (A) and tidal change (B) and on fish presence or absence measured at 30 deployments in the southern California Bight over 24 hour periods.



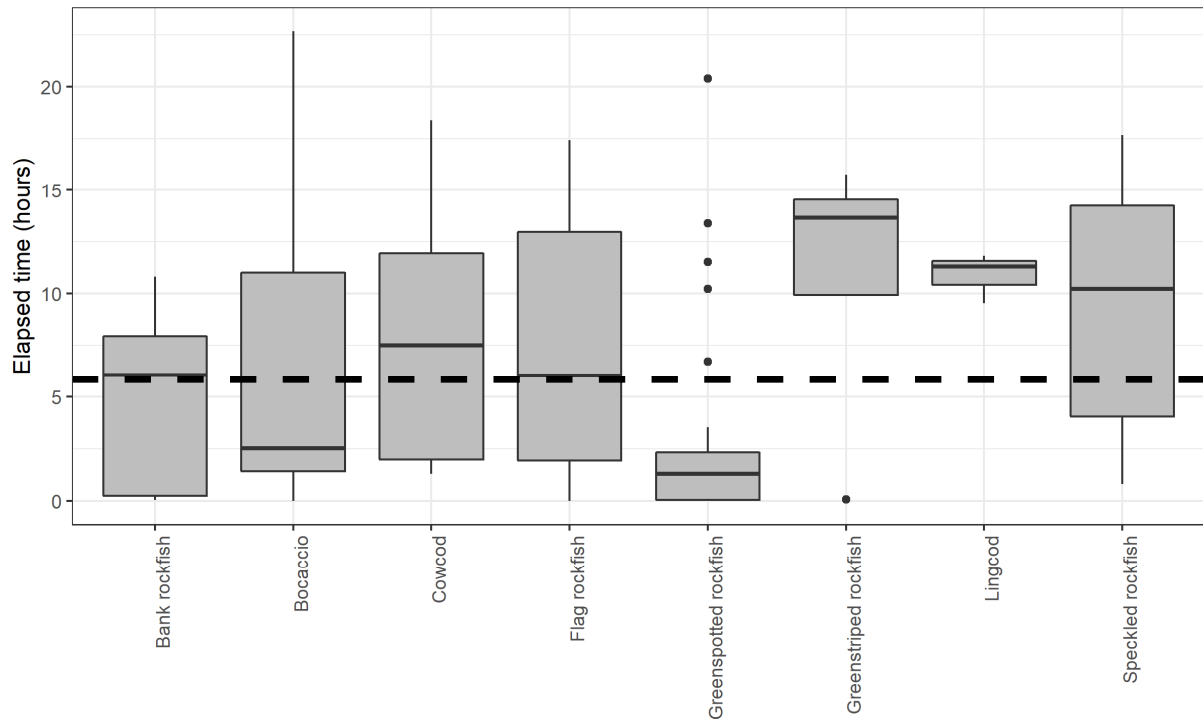
704
705
706
707
708
709
710
711
712
713

Figure 5. Density of rockfishes and lingcod recorded by time of day during 30 stationary camera deployments in the southern California Bight. Data are smoothed using a Loess smoother (standard errors of the smooth are represented by grey shading for each line). Purple shaded areas indicate local hours of nighttime and pink shaded areas indicate the hour surrounding dawn and dusk. Densities are scaled to 1 for each species to facilitate graphical representation.



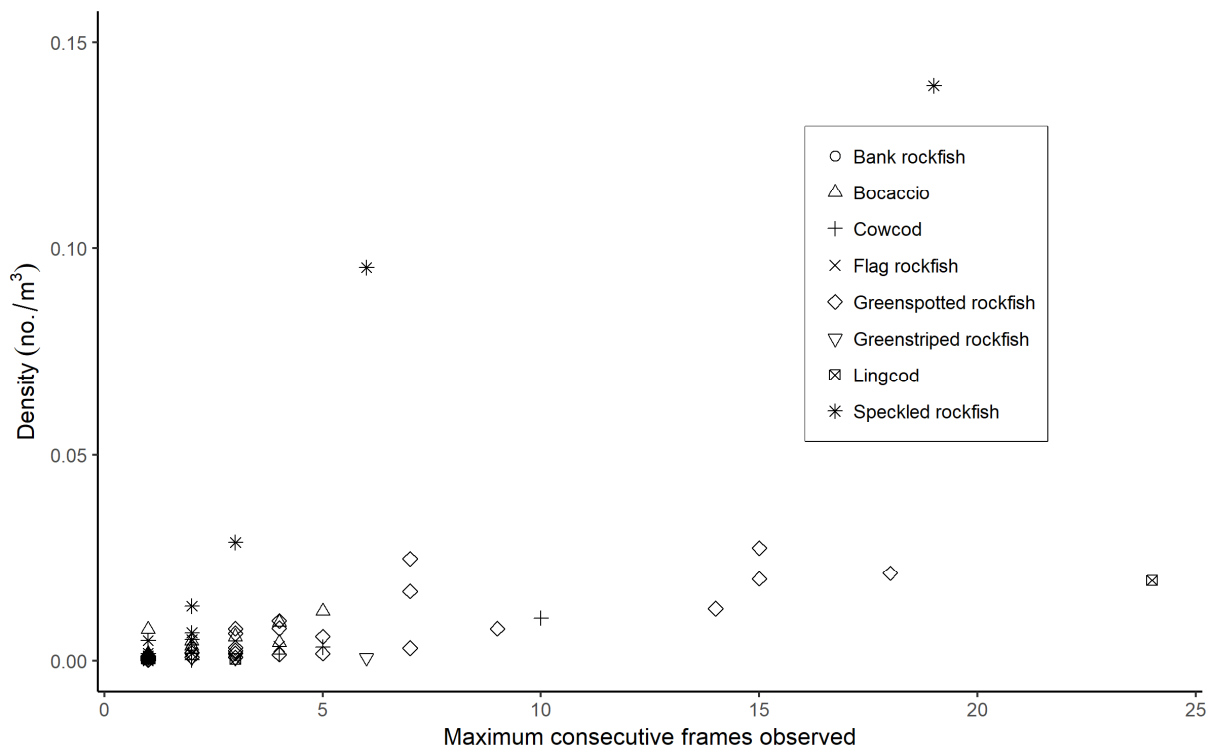
714
 715
 716
 717
 718
 719
 720

Figure 6. Variability of fish in same deployment over time since the deployment in 10-minute intervals (A) and the relationship between mean density and the standard deviation of the mean for those same intervals since deployment (B).



721
 722
 723
 724
 725
 726
 727
 728

Figure 7. Elapsed time between deployment and first arrival of fish (by species) across 30 deployments of stationary cameras in the southern California Bight. The orange dashed line indicates the average elapsed time until daylight (1/2 hour after sunrise). Lines inside the colored boxes indicate median values and the height of the box corresponds to the 1st and 3rd quartiles of the data. Outliers are shown as individual points.



729
730
731
732
733
734
735
736
737

Fig. 8. Density of fish for TrigCam deployments versus the maximum number of consecutive frames in which fish of that species were observed. Data are from 30 deployments of TrigCams on the Footprint Bank in 2017 during daylight hours.

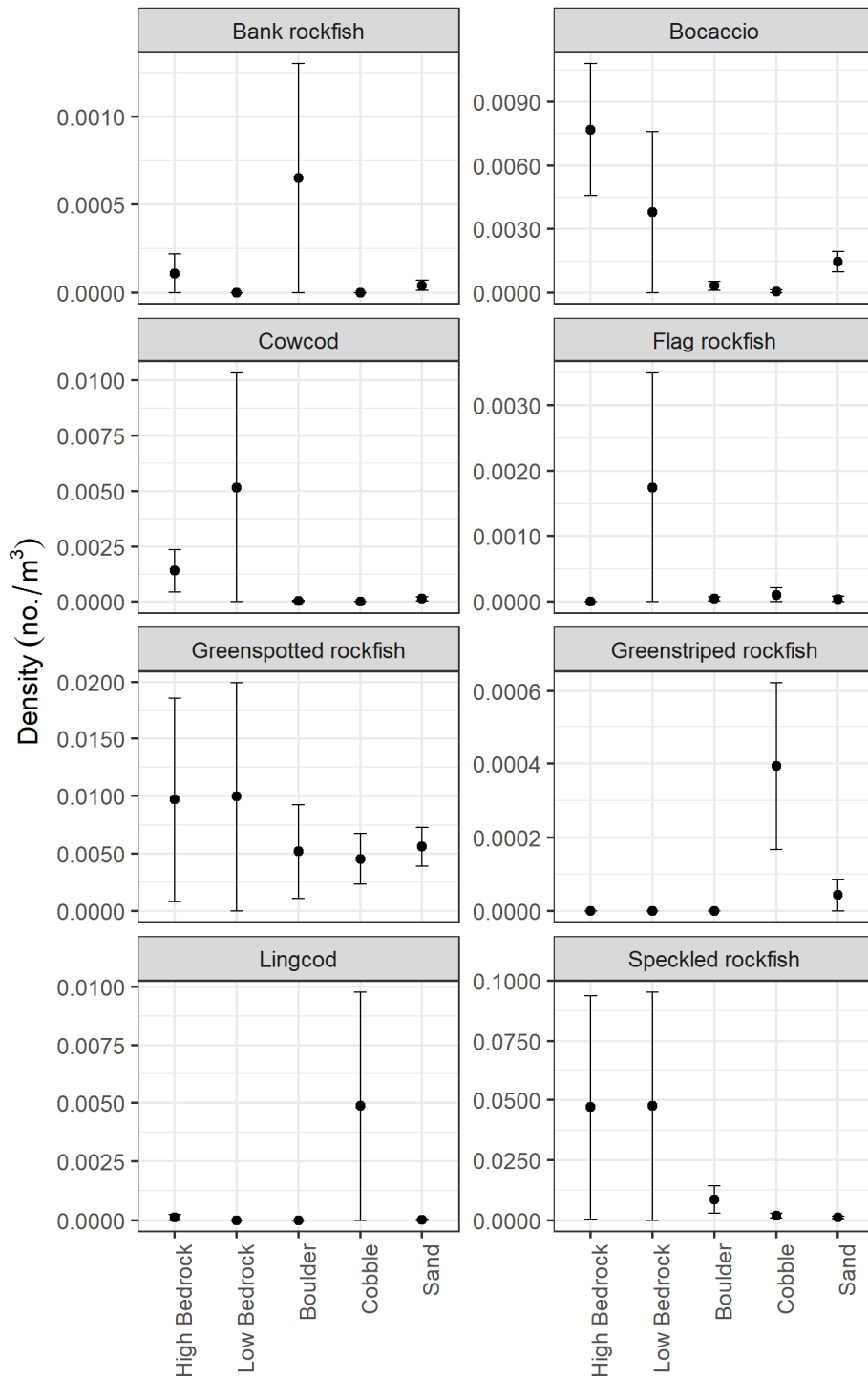
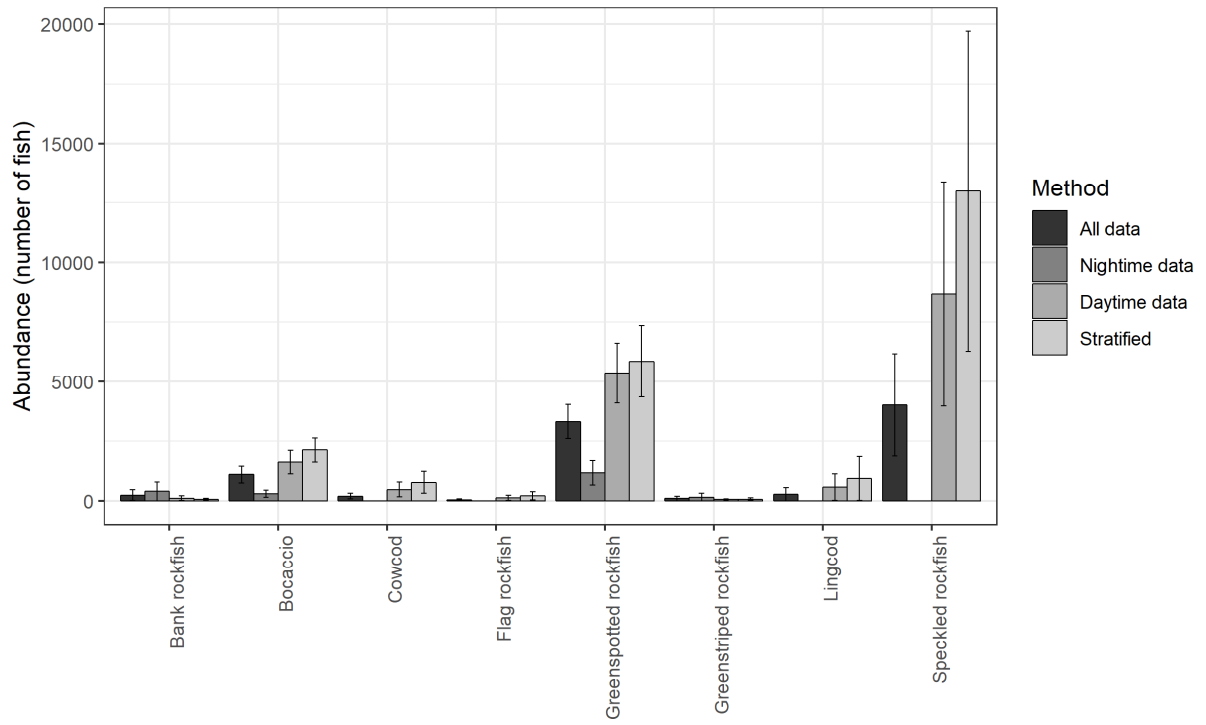


Fig. 9. Density of fish by primary substrate type and standard error bars for TrigCam deployments on the Footprint Bank in 2017.

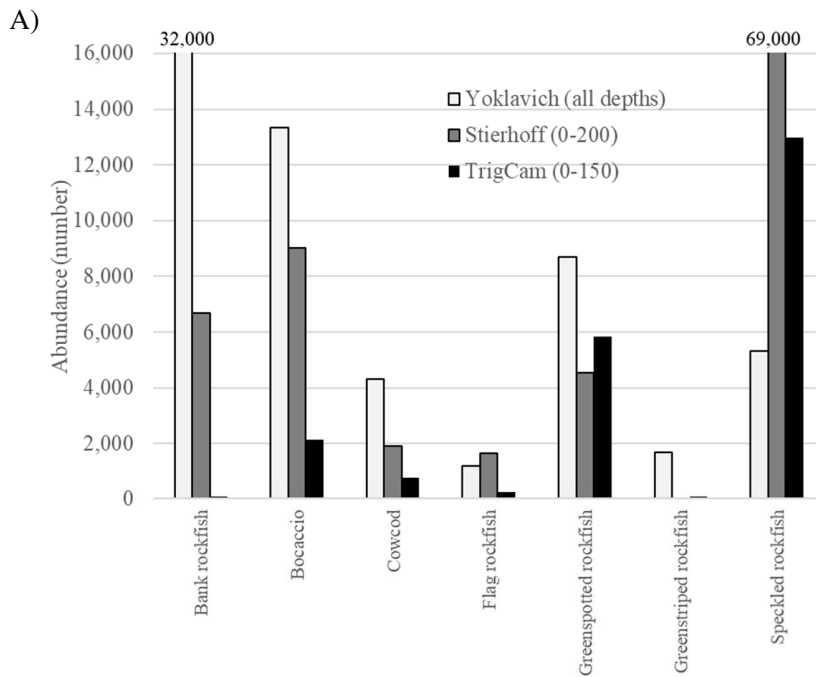
738
739
740
741



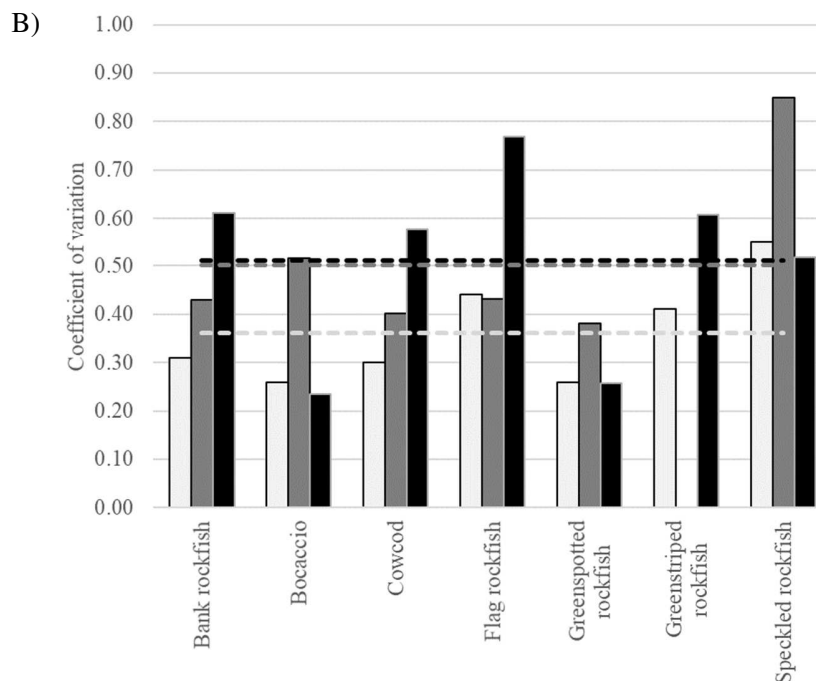
742
 743
 744
 745
 746
 747
 748

Fig. 10. Estimated abundance and standard error bars of rockfishes from Footprint Bank from TrigCam data in 2017 with four methods to calculate the abundance; 1) all data combined, 2) nighttime only, 3) daytime only, and 4) daytime only and stratified by primary substrate type.

749



750



751

752

753

754

755

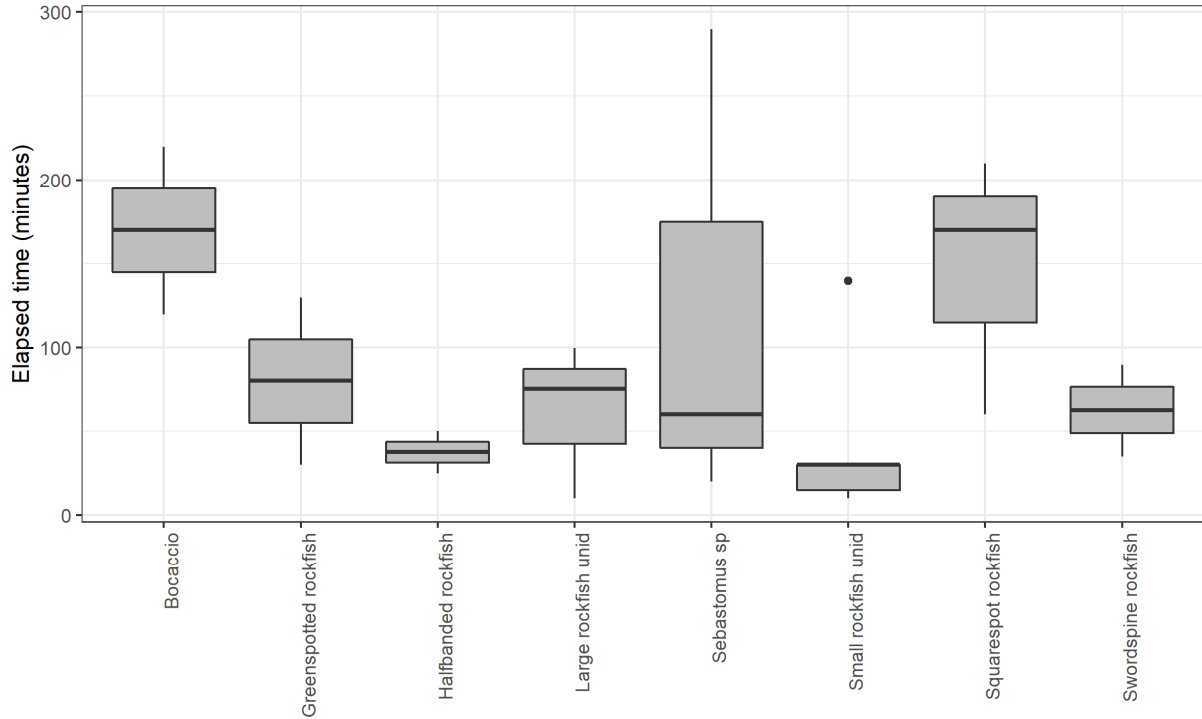
756

757

758

Figure 11. Abundance estimates (A) and coefficients of variation (B) of rockfishes from this study (TrigCam) at depths to 150 m, the Stierhoff et al. 2012 study of Footprint Bank (from transects to depths of 200 m) and the Yoklavich et al. 2013 study (at depths to 400 m) at Footprint Bank. The bars are abundance estimates for the Footprint Bank (in numbers of fish) and the lines are coefficients of variation for those estimates of abundance. The dashed lines are the corresponding average CV across rockfish species. Two abundance estimates were truncated in (A) above, with the estimate shown as numbers at the top of the bar.

759
760
761



762
763
764
765
766
767
768
769
770
771

Figure S1. Elapsed time between first contact with the seafloor and first observation of rockfish by species or species group. The data are averages for 5 deployments conducted in 2016 where the TrigCam was shooting images when it reached the seafloor and the deployment was made prior to 13:00. The average elapsed time across all species was 87 minutes (sd = 78). Species was not significant ($p = 0.41$) and when species were combined into large and small species, there were no differences observed.